A geomagnetic precursor to the 1979 Carlisle earthquake

Beamish, D., 1982. A geomagnetic precursor to the 1979 Carlisle earthquake. Geophys. J. R. astr. Soc., 68, 531-543.

DOI: 10.1111/j.1365-246X.1982.tb04913.x

Corresponding author:

David Beamish

British Geological Survey, Keyworth, Nottingham, NG12 5GG, UK

Email: D.Beamish@bgs.ac.uk

Tel: 0115 936 3432

Fax: 0115 936 3261

Summary

A study of horizontal field transfer functions, in the period range 10-10^4 s, has been made for the 2 year period preceding the 1979 Carlisle earthquake (magnitude 5). The study using two sites, local to and remote from the earthquake epicentre, reveals that a precursory effect is observed at short periods (< 102 s) some 35 km from the main epicentre. The results indicate a change from two-dimensional geolectric anisotropy to a more conductive three-dimensional geoelectric configuration during the period immediately preceding the earthquake.

Introduction

Present studies of earthquake mechanisms involve the measurement of a number of diagnostic Earth properties such as tilt, strain, radon emission, seismic velocities and electrical resistivity. A list of 19 such properties which have been related to earthquake occurrence has been compiled (Rikitake 1979). The temporal variations in one or more of these properties, and their inter-relation, allow models of earthquake mechanisms to be developed. The physical processes involve rock failure and almost all currently proposed models involve the response of microcracks to the changing levels of stress in an earthquake preparation zone. Such models (Brady 1975) also attempt to account for a number of precursory phenomena that are observed prior to failure. The term precursor is applied to a variation in one or more of the above parameters which either directly or indirectly indicates that the process leading to failure has begun.

The model of stress-induced dilatancy (Nur 1972) has had some success in explaining the variation of a number of independent geophysical parameters prior to seismic events (Scholz, Sykes & Aggarwal 1973). Dilatancy is the non-elastic increase in volume caused by stress, depending not only on the applied stress, but also on the rate of stress accumulation (Brace, Paulding & Scholz 1966). The phenomena is well- documented by laboratory studies on crystalline rocks (Brace et al. 1966; Brace & Orange 1968). The volume increase in stressed rock produces a large increase in effective porosity (Brace & Orange 1968) and permeability (Brace 1978). Even in partially saturated rock these changes can produce significant changes in electrical resistivity (Madden 1978). The total resistivity of crustal material is the sum of the effects of conduction in the solid matrix and conduction along pores and cracks containing electrolytic fluid. At modest temperatures the fluid effect is dominant (Brace & Orange 1968; Olhoeft 1981). In the absence of crack porosity, the resistivities of a remarkably wide range of rock types are related to porosity by Archies Law:

$$\rho / \rho_f = \eta^{-m}$$

where ρ is the rock resistivity, ρ_f is the pore-fluid resistivity, η is the porosity and m is an empirically determined constant generally between 1 and 2. In the case where m = 1, fractional change in porosity equals minus the fractional change in resistivity, although the application of the above scalar relationship would be inappropriate to the anisotropic strain and resistivity variations actually encountered. The overall sensitivity of electrical properties to stress changes depends on the extent to which cracks control the electrical resistivity. Summarizing a large volume of laboratory work undertaken at MIT on the resistivity-stress relationships of igneous, metamorphic and sedimentary rocks, Madden (1978) suggests that amplification factors ($\%\Delta\rho/\Delta\mu$), where μ is a strain of between 100 and 200 and stress sensitivities ($\Delta\rho$ bar^{-1}) of between 0.05 and 0.4 may be encountered in crustal dilatant zones. The exceptional amplification factors of between 103 and 105 reported by Yamazaki (1965) of tuffaceous rocks from the Izu Peninsula have since been confirmed for partially saturated California tuffs (Morrow & Brace 1981).

Resistivity is not measured directly but rather by active or passive electromagnetic soundings, in which instance the resistivity is termed apparent. The apparent resistivity measurements of Barsukov Barsukov (1972), Mazella & Morrison (1974) and Yu-Lin & Fu-Ye (1978) have provided clear evidence of time-dependent changes in apparent resistivity that correlate with seismic events. A number of

other time-dependent electromagnetic response functions that have been associated with earthquakes have been reviewed (Rikitake 1976a; Niblett & Honkura 1980). Although some measurements have provided positive correlations, the situation with regard to geomagnetic transfer function measurements is more uncertain. It has been pointed out (Niblett & Honkura 1980) that accurately recorded difference fields between pairs of stations (local and remote) should allow a better assessment of the possible time-dependence of transfer functions within a locally anomalous region. In addition, electromagnetic induction in a hypothetical dilatant crustal zone, giving rise to an order of magnitude decrease in resistivity, has been modelled (Rikitake 1976b). Using the appropriate induction parameters it was found that enhancements of the horizontal field of up to 100 per cent might be expected for short period (< 100 s) events.

A study of inter-station horizontal field transfer functions between Eskdalemuir (ESK, Fig. 1) and York during 1978 and 1979 has revealed that a significant time-dependence is observed at short periods prior to the Carlisle earthquake (M = 5) which occurred on 1979 December 26 (Boxing Day).

The earthquake and geoelectric setting

The Boxing Day Earthquake (BDE) occurred in the vicinity of Carlisle (Fig. 1) following a foreshock sequence now apparent from data recorded by the LOWNET seismic stations of southern Scotland (Nielson 1980). A fault plane solution based on aftershock data has been reported by King (1980). Hypocentral depths range from 3 to 12 km, within the Silurian, and cluster around 7 km. The data indicate that the BDE could be accounted for by 30 cm of slip along one or more thrust planes some 3.5 km in diameter, assuming a typical stress drop of 30 bar. It was also noted (King 1980) that the BDE was located along a proposed strike direction of the Palaeozoic Iapetus suture zone.

Previous (Edwards, Law & White 1971; Bailey & Edwards 1976) and current geomagnetic induction studies have identified the Southern Uplands and Northumberland Basin as being underlain by a region of low integrated resistivity at lower crustal depths. It has been suggested (Bailey & Edwards 1976) that the low resistivity can be directly related to the presence of hydrated Late Palaeozoic oceanic crust underlying the Southern Uplands. More recent magnetotelluric studies (Jones & Hutton 1979a, b) have provided geoelectric models for sites in Southern Scotland. Of particular relevance is the one- dimensional model obtained at NEW (Fig. 1). The results indicate a resistive upper crustal layer (base 16-36 km) underlain by a conducting lower crustal/upper mantle region of resistivity 25-90 ohm.m. Upper crustal structure is unresolved by the long-period variations used in these studies.

Data and analysis

The geomagnetic data used in this analysis came from two high-resolution magnetometers that have operated since 1976 at Eskdalemuir (ESK) and York (YOR). The geographical coordinates are, ESK: 55.32 N and 356.80 E and YOR: 53.95 N, 358.95 E. The observatory at ESK is situated some 35 km from the main epicentre of the BDE (Fig. 1). The instruments are three-axis rubidium vapour magnetometers with a sampling interval of 2.5 s and a resolution of the order of 0.025 nT (Riddick, Brown & Forbes 1976). The data are recorded digitally on cassette and subsequently transcribed into computer compatible format. The data set is not continuous; data gaps exist every 3-4 day due to cassette change. A timing accuracy of better than 100ms is maintained at each site.

In the case of geomagnetic fields we attempt to separate the total field components (Ti) into normal (Ni) and anomalous (Ai) parts, with Ti = Ni + Ai. The normal part includes contributions from external inducing fields and from currents flowing in a normal layered earth. The anomalous part then includes only contributions from lateral discontinuities in geoelectric structure. We may write

$\mathbf{A}_i = \mathbf{K}_{ij}\,\mathbf{N}_i + \boldsymbol{\varepsilon}_j$

where $\boldsymbol{\varepsilon}_j$ is an error term which is minimized in the determination of the induction tensor $\mathbf{K}_{ij}$ (Schmucker 1970). For a general uniform inducing field it has been argued (Lilley 1974) that at a point near a lateral discontinuity, the induction tensor possesses a simple degeneracy such that

$$\mathbf{K} = \begin{bmatrix} K_{11} & K_{12} & 0 \\ K_{21} & K_{22} & 0 \\ K_{31} & K_{32} & 0 \end{bmatrix}.$$

Techniques exist for the determination of the vertical field transfer function (K_{31} , K_{32}) when only one station is available (Banks 1973). The determination of the other four elements requires inter-station techniques. When a suitable reference station exists, it is possible to relate the two horizontal horizontal components recorded at a site (S) to those at the reference site (R). At a particular frequency we may write

$$H_x^{\mathrm{A}} = H_x^{\mathrm{S}} - H_x^{\mathrm{R}} = C \cdot H_x^{\mathrm{R}} + D \cdot H_y^{\mathrm{R}} + \epsilon_x \qquad (1)$$

$$H_y^{\mathrm{A}} = H_y^{\mathrm{S}} - H_y^{\mathrm{R}} = E \cdot H_x^{\mathrm{R}} + F \cdot H_y^{\mathrm{R}} + \epsilon_y \qquad (2)$$

where the superscript A refers to the anomalous part. Provided the separation between the two sites is less than the scale length of the inducing field, the transfer functions (C, D) and (E, F) provide a measure of the anomalous horizontal fields recorded at the two sites, S and R. If site R can be classified as normal, the transfer functions defined in (1) and (2) become (K_{11} , K_{12}) and (K_{21} , K_{22}) as defined above. It is worth noting that the subtraction of a reference component is not strictly required (Schmucker 1970). The correlation can be performed using (H^S_x, H^S_y) as recorded at site S. Such a procedure would result in transfer functions (C', D ') and (E', F') that include contributions from current flow in a layered earth. The procedure used provides transfer functions (C, D) and (E, F) that are due to anomalous current flow along lateral variations in geoelectric structure.

In order to provide stable and accurate transfer function estimates, a certain minimum number of degrees of freedom are required. Previous investigations (Beamish 1979) have demonstrated that, for the methods of analysis employed, approximately 5 x 24 hr records are required at the latitude of this study. The data sets should also be evenly distributed in local time (Beamish 1980). In order to investigate time-dependent effects in transfer functions over the 2 yr period 1978-79, the following four-part data selection scheme was adopted. (a) In any given calendar month, 5 x 24 hr of simultaneous data had to be available at the two sites. (b) Each 24 hr record had to run from 00.00-24.00 LT. (c) In order to avoid data extremes, the 5 IDD and 5 IQD for each calendar month were excluded. (d) All data records and difference fields used in the analysis were plotted and incorrect data records rejected.

The above criteria were strictly adhered to with the result that certain months provided insufficient records for analysis due mainly to instrument malfunctions at one or both magnetometer sites. The greater availability of good data towards the end of 1979 provided increased temporal resolution.

Effect of site separation

The effect of the N- S site separation of 210 km between ESK and YOR was investigated using induction arrows which derive from the vertical field transfer function (K_{31} , K_{32}) (Schmucker 1970). Induction arrows allow the complex response (K_{31} , K_{32}) to be presented in terms of amplitude and an azimuth which defines the normal to the strike of a local geoelectric boundary. Two such responses are defined for vertical fields responding in-phase (real) and in-quadrature (imaginary) with the appropriate horizontal field vector.

Induction arrows were computed for two cases using the same 5 x 24 hr of data selected according to the above scheme. In the first instance, the induction arrows were calculated using the vertical field at ESK with the horizontal field components recorded locally at ESK. The results, as a function of period, are shown in Fig. 2(a). In the second case, the analysis was repeated using the vertical field at ESK with the horizontal field components recorded remotely at YOR. The results are shown in Fig. 2(b). A comparison of the two sets of results reveals that both amplitudes and azimuths for in-phase and in-quadrature determinations are equivalent at the 95 per cent confidence level throughout the period range of the analysis. The results argue that the use of reference horizontal fields recorded at YOR will also be appropriate to the determination of the horizontal field transfer functions (C, D) and (E, F) in the period range 10-104 s.

Horizontal field results

A determination of the transfer function (C, D), (E, F) is shown in Fig. 3 in terms of real (Re) and imaginary (Im) parts of the four complex functions of period. The data are centred on day 310, some 50 days prior to the BDE. The results clearly demonstrate that large anomalous horizontal fields are present at short periods in the real (Re) parts of C and F. Significantly non-zero determinations are also present in the other phases and functions.

To simplify presentation, four period bands were chosen to represent the period range of the analysis; these were B3 (4000-2000 s), B7 (I000-600 s), B11 (250-150 s) and B15 (70-50 s). In the following diagrams the day number of each determination refers to the mean of the five day numbers used in the determination. The BDE is shown as the broken vertical line on day 360 1979.

A consequence of electromagnetic induction in an earth possessing lateral anisotropy (Jones & Price 1970) is that the transfer functions D, relating the anomalous Hx component to regional N-S current flow, and E, relating the anomalous Hy component to regional E-W current flow, are small in relation to both C and F. As noted above, the analysis confirms small, though non-zero, values for both D and E. We here present results for C and F corresponding to an E-polarization condition (Jones & Price 1970) which generates the largest anomalous horizontal fields.

The behaviour of the real (Re) and imaginary (Im) parts of C during 1978 and 1979 are shown in Fig. 4(a and b respectively). It is apparent that at long periods (B3 and B7) a relatively stable response is observed throughout the period. Re (C), however, exhibits two distinct effects particularly in the shortest period band (B 15). The first effect is a long-term increase in the magnitude of Re (C) from

day 0 1978 to day 300 1978. This increase is followed by a period of partial recovery to smaller values. A second effect occurs in the latter half of 1979. A large and rapid excursion begins after day 200 reaching a maximum on day 294 1979. This second effect is followed by a period of partial recovery prior to the BDE. The imaginary part of C (Fig. 4b) is much more stable throughout the period though a significant time-dependence is observed in the latter half of 1979. An excursion occurs with Im (C) decreasing in magnitude until a minimum occurs on day 294 1979 corresponding to the time of maximum excursion of Re (C).

The behaviour of the real and imaginary parts of F, relating the anomalous Hy component to regional N-S current flow, are shown in Fig. 5(a and b respectively). In contrast to Re (C), Re (F) does not exhibit a long-term trend during 1978. In accord with the behaviour of Re (C), however, Re(F) undergoes a rapid excursion after day 200 1979, reaching a maximum on day 294 1979 at periods < 250 s. A further oscillation is observed prior to the BDE, corresponding to the one observed in Re (C). In contrast to Re (C) at long periods (B3 and B7), Re (F) undergoes a rapid excursion immediately after the BDE. The imaginary part of F (Fig. 5b) is relatively stable throughout the 2 yr period. Again correlating with the behaviour of Im (C), Im (F) reaches a minimum value on day 294 1979 although the excursion is by no means as large as that observed in Im (C).

In discussing the time-dependent effects observed we must make the implicit assumption that the behaviour of C and F relates to time-dependent changes in the internal current system in the vicinity of ESK and that any such changes do not occur at the reference site YOR. Given this assumption, the analysis appears to have identified significant temporal changes in the anomalous horizontal fields recorded at ESK prior to the BDE. The main features of the observed time-dependence can be summarized as follows. At periods < 250 s, both Re (C) and Re (F) experience a large excursion after day 200 1979 and reach maximum values on day 294 1979, some 66 days prior to the BDE. Also at this time the imaginary parts of both C and F tend to minimum values thereby creating a largely in-phase response at the time of maximum anomalous horizontal field. There is considerable detail in the temporal effects immediately prior to the BDE. Following the occurrence of maximum horizontal field both in-phase components Re(C) and Re(F) undergo a partial recovery that indicates a further oscillation in the behaviour of the anomalous horizontal fields recorded at ESK.

Changes in the geoelectric configuration

Once determined the complex transfer functions (C, D) and (E, F) can be used to define both directional and dimensional indicators of geoelectric structure (Lilley 1974). Several methods of presentation exist which display the anomalous magnetic field response to normal or regional horizontal fields. To summarize the response of both H^A_x and H^A_y at ESK we assume a regional horizontal field H^R at YOR with azimuth θ_R which results in an anomalous horizontal field H^A with azimuth θ_s at ESK. The regional and anomalous horizontal fields are then defined by $H^R_x = H^R \cos\theta_R$, $H^R_y = H^R \sin\theta_R$, $H^A_x = H^A \cos\theta_s$ and $H^A_y = H^A \sin\theta_s$. Using (1) and (2) we can then define the amplitude of the anomalous horizontal field vector at ESK as

$$(H^A)^2 = (C^2 + E^2)\cos^2\theta_R + (D^2 + F^2)\sin^2\theta_R + (C^2 D^2 + E^2 F^2)\sin 2\theta_R \qquad (3)$$

where H^R has been defined with unit amplitude and zero phase. Similarly the azimuth of the θ_A vector is given by

$\tan \theta_A = (E + F \tan\theta_R) / (C + D \tan\theta_R)$

Using (3), two ellipses of rotation are obtained by plotting at azimuth θ_R , two radii inversely proportional to the real and imaginary parts of H^A. Alternatively, we may plot two radii directly proportional to the real and imaginary parts of H^A at the local azimuth θ_A. The second method is the more readily interpreted since ellipse dimensions are directly proportional to the anomalous field in the principal directions.

Fig. 6(a, b) displays the in-phase rotation ellipses obtained from data centred on day 063 1979 (Fig. 6a) and secondly from data centred on day 310 1979 (Fig. 6b), when a major excursion in Re (C) and Re (F) occurs. Referring to the shortest period (B 15) in which the largest precursory excursions are apparent we note that in early 1979 (Fig. 6a) the anomalous horizontal field response at ESK is approximately two-dimensional; the strike direction of conductive anisotropy and anomalous current flow being normal to the major axis of the rotation ellipse (142° geographic, Fig. 6a). It is worth noting that a strike direction of 52° is consistent with late Palaeozoic strike-slip movements in the region of the Solway Firth (Phillips, Stillman & Murphy 1976), and the major Caledonian trends of the region. During the period immediately prior to the BDE (Fig. 6b) the preferential direction of response maximization disappears at short periods. Such behaviour suggests a distinct change from a two-dimensional geoelectric configuration to a more conductive three- dimensional configuration during the period immediately preceding the BDE.

Comparing Figs 6(a) and 6(b), it is apparent that the largest increase in the horizontal field vector occurs in a direction parallel to the strike direction of 52°. The largest increase in anomalous current is therefore directed normal to the strike direction although a significant increase in anomalous current is also observed along the strike direction.

Discussion

It is clear from the results obtained that a dense network of stations would be required to interpret the detailed behaviour of the anomalous horizontal fields recorded at ESK. Any interpretation of the observed time-dependence is further restricted due to the lack of additional geophysical/geochemical observations prior to the BDE. The following discussion relates entirely to the observation that changes in the geoelectric configuration, as deduced from the anomalous horizontal fields at ESK, precede the BDE.

Several possible mechanisms have been proposed which could account for the observed time-dependence (Rikitake 1976a). It appears difficult to account for the observed magnitude of the enhanced fields entirely in terms of the effects of conduction in the solid phase. The low integrated resistivity beneath the Southern Uplands has already been noted. The implications of such low resistivities (< 100 ohm.m) at lower crustal depths have recently been discussed by Ohloeft (1981). It appears likely that free-water saturation of a few weight per cent are required to explain such values. It is also apparent from the laboratory work that from room temperature through to granitic melting (650-1100 °C) changes of several weight per cent water are capable of producing decreases in electrical resistivity of between 3 and 9 orders of magnitude.

The mechanism of stress-induced dilatancy (Nur 1972) predicts an order of magnitude decrease in the electrical resistivity of water saturated silicate rocks after the onset of pore dilation, within a

closed system. Pore dilation in laboratory samples occurs at between1/3 to 2/3 of the fracture stress (Brace & Orange 1968), and it is apparent that the average stress drop associated with most earthquakes (< 200 bar) would be insufficient to initiate dilatancy in the competent laboratory samples. At the present time, most laboratory work has studied the effect of microcrack (cf. joint) dilatancy. When an earthquake occurs along well-established faults, the relevant cracks are likely to be joints and large scale fractures. In such a heterogeneous fault zone, the stress field is unlikely to be be uniformly distributed. Recent detailed studies (Wyss, Johnston & Klein 1981) have revealed the presence of localized and dilatant regions of high stress within an earthquake preparation zone.

Direct observations of crack behaviour (dilatant-induced and pre-existing) under stress (Hadley 1975; Batzle, Simmons & Siegfried 1980) have revealed that stress-induced cracks are non-randomly orientated with the plane of the induced crack close to the axis of maximum compressive stress. It has been argued that such stress-induced cracks will appear anisotropic to short-period seismic waves (Crampin & McGonigle 1981). The symmetry directions of large-scale dilatancy should also introduce modifications to geoelectric structure in the principal directions of crustal stress accumulation. Subsequent fluid diffusion (when it occurs) will be governed by the overall pore pressure gradients generated by the dilatant volume. When two models (wet and dry) of earthquake precursor mechanisms are compared (Mjachkin et al. 1975) it is predicted that during an anomalous period, maximum resistivity decrease should occur in a direction parallel with the eventual fault plane (dry model) or inclined to it, in the case of a wet dilatancy-diffusion mechanism. It is clear from the results shown in Fig. 6 (a, b) that, with regard to the fault plane solution obtained for the BDE (King 1980), the direction of maximum anomalous current increase is inclined to the fault plane thus favouring a dilatancy-diffusion interpretation. It is apparent from the results presented in Figs 4(a) and 5(a) that predominantly N-S anomalous currents affecting the anomalous Hy component at long periods (B3 and B7) occur after the BDE. Such behaviour may again be compatible with a dilatancy-diffusion interpretation. If pore fluid is present in microcracks, post-dilatant recovery (crack closure) will be governed by the rate at which fluid can be expelled. Temporal variations in electrical resistivity are indeed anticipated during dilatancy recovery (Scholz & Kranz 1974) although the reason why only the anomalous horizontal fields of long periods (> 600 s) are affected, remains unclear. The persistence of anomalous horizontal fields of long periods after an earthquake occurrence has previously been noted in the results of Rikitake et al. (1980).

While this study allows a geomagnetic precursor to be defined, albeit in hindsight, the lack of additional control does not allow possible earthquake mechanisms to be investigated in detail. A strong aftershock sequence in the region is currently being monitored. It would be of interest to extend this study onwards in time to investigate further geomagnetic effects during the recovery period.

Acknowledgment

This study is published with the approval of the Director, Institute of Geological Sciences (NERC).

References

Bailey, R. C. & Edwards, R. N., 1976. The effect of source field polarisation on geomagnetic variation anomalies in the British Isles, *Geophys. J. R. astr. Soc.,* 45, 97-104.

Banks, R. J., 1973. Data processing and interpretation in geomagnetic deep sounding, *Phys. Earth planet. Int.,* 7, 339-348.

Barsukov, 0. M., 1972. Variations of electric resistivity of mountain rocks connected with tectonic causes, *Tectonophys.,* 14, 273-277.

Batzle, M. L., Simmons, G. & Siegfried, R. W., 1980. Microcrack closure in rocks under stress: direct observation, *J. geophys. Res.,* 85, 7072-7090.

Beamish, D., 1979. Source field effects on transfer functions at mid-latitudes, *Geophys. J. R. astr. Soc.,*58, 117-134.

Beamish, D., 1980. Diurnal characteristics of transfer functions at pulsation periods, *Geophys. J. R. astr. Soc.,* 61, 623-643.

Brace, W. F., 1978. A note on permeability changes in geologic material due to stress, *Pure appl. Geophys.* 116, 627-633.

Brace, W. F. & Orange, A. S., 1968. Further studies of the effects of pressure on electrical resistivity of rocks, J. *geophys. Res.,* 73, 1433-1445.

Brace, W. F., Paulding, B. W. & Scholz, C. H., 1966. Dilatancy in the fracture of crystalline rocks, *J. geophys. Res.,* 71, 3939-3953.

Brady, B. T., 1975. Theory of earthquakes II. Inclusion theory of crustal earthquakes, *Pure appl. Geophys.,* 113, 149-168.

Crampin, S. & McGonigle, R., 1981. The variation of delays in stress-induced anisotropic polarization anomalies, *Geophys. J. R. astr. Soc.,* 64, 115-131.

Edwards, R. N., Law, L. K. & White, A., 1971. Geomagnetic variations in the British Isles and their relation to electrical currents in the ocean and shallow seas, *Phil. Trans. R. Soc. A,* 270, 289-323.

Hadley, K., 1975. Azimuthal variation of dilatancy*, J. geophys. Res.,* 80, 4845-4850.

Jones, A. G. & Hu tton, R., 1979a. A multi-station magnetotelluric study in southern Scotland I. Field- work, data analysis and results, *Geophys. J. R. astr. Soc.,* 56, 329-349.

Jones, A. G. & Hutton, R., 1979b. A multi-station magnetotelluric study in southern Scotland II. Monte- Carlo inversion of the data and its geophysical and tectonic implications, *Geophys. J. R. astr. Soc.,* 56, 351-368.

Jones, F. W. & Price, A. T., 1970. The perturbations of alternating geomagnetic fields by conductivity anomalies, *Geophys. J. R. astr. Soc.,* 20, 317-334.

King, G., 1980. A fault plane solution for the Carlisle earthquake, 26 December 1979, *Nature,* 286, 142-143.

Lilley, F. E. M., 1974. Analysis of the geomagnetic induction tensor, *Phys. Earth planet. Int.,* 8, 301-316.

Madden, T. M., 1978. Electrical measurements as stress-strain monitors, Proceedings of Conference VII, Stress and strain measurements related to earthquake prediction, *Geol. Surv. Open File Rep. U.S.,* 79-370.

Mazella, A. & Morrison, H. F., 1974. Electrical resistivity variations associated with earthquakes on the San Andreas fault, *Science,* 185, 855-857.

Mjachkin, V. I., Brace, W. F., Sobolev, G. A. & Dieterich, J. H., 1975. Two models for earthquake fore-runners, *Pure appl. Geophys.,* 113, 169-181.

Morrow, C. & Brace, W. F., 1981. Electrical resistivity changes in tuffs due to stress, *J. geophys. Res.,* 86, 2929-2934.

Niblett, E. R. & Honkura, Y., 1980. Time-dependence of electromagnetic transfer functions and their association with tectonic activity, *Geophys. Surv.,* 4, 97-114.

Nielson, G., 1980. The recent Carlisle area earthquakes, *Edinburgh. Geol.,* March, 20-25.

Nur, A., 1972. Dilatancy, pore fluids, and premonitory variations of t_s/t_p travel times, *Bull. seism. Soc. Am.,* 62, 1217-1222.

Olhoeft, G. R., 1981. Electrical properties of granite with implications for the lower crust, *J. geophys. Res.,* 86, 931-936.

Phillips, W. E. A., Stillman, C. J. & Murphy, T., 1976. A Caledonian plate tectonic model, *J. geol. Soc. London,* 132, 579-609.

Riddick, J. C., Brown, J. & Forbes, A. *1.,* 1976. A low power movable observatory unit for magneto-meter array application, *Inst. geol. Sci. Geomagn. Unit, Int. Rep. No. 17.*

Rikitake, T., 1976a. Earthquake prediction, *Developments in Solid Earth Geophysics, Vol. 9,* Elsevier, Amsterdam.

Rikitake, T., 1976b. Crustal dilatancy and geomagnetic variations of short period, *J. Geomagn. Geo- elect.,* 28, 145-156.

Rikitake, T., 1979. Classification of earthquake precursors, *Tectonophys.,* 54, 293-309.

Rikitake, T., Honkura, Y., Tanaka, H., Ohshiman, N., Sasai, Y., Ishikawa, Y., Koyama, S., Kawamura, M. & Ohchi, K., 1980. Changes in the geomagnetic field associated with earthquakes in the Izu Peninsula, Japan,]. *Geomagn. Geoelect.,* 32, 721- 739.

Schmucker, U. 1970. Anomalies of geomagnetic variations, *Bull. Scripps 1nstn Oceanogr. 13.*

Scholz, C. H., Sykes, L. R. & Aggarwal, Y. P., 1973. Earthquake prediction: a physical basis, *Science,* 181, 803-810.

Scholz, C. H. & Kranz, R., 1974. Notes on dilatancy recovery *, J. geophys. Res.,* 79, 2132-2135.

Wyss, M., Johnston, A. C. & Klein, F. W., 1981. Multiple asperity model for earthquake prediction, *Nature,* 289, 231-234.

Yamazaki, Y., 1965. Electrical conductivity of strained rocks, 1. Laboratory experiments on sedimentary rocks, *Bull. Earthq. Res., Inst. Tokyo Univ.,* 43, 783-790.

Yii-Lin, Z. & Fu-Ye, Q., 1978. Electrical resistivity anomaly observed in and around the epicentral area prior to the Tangshan earthquake of 1976. *Acta geophys. sin.,* 21, 181-190 (in Chinese with English abstract).

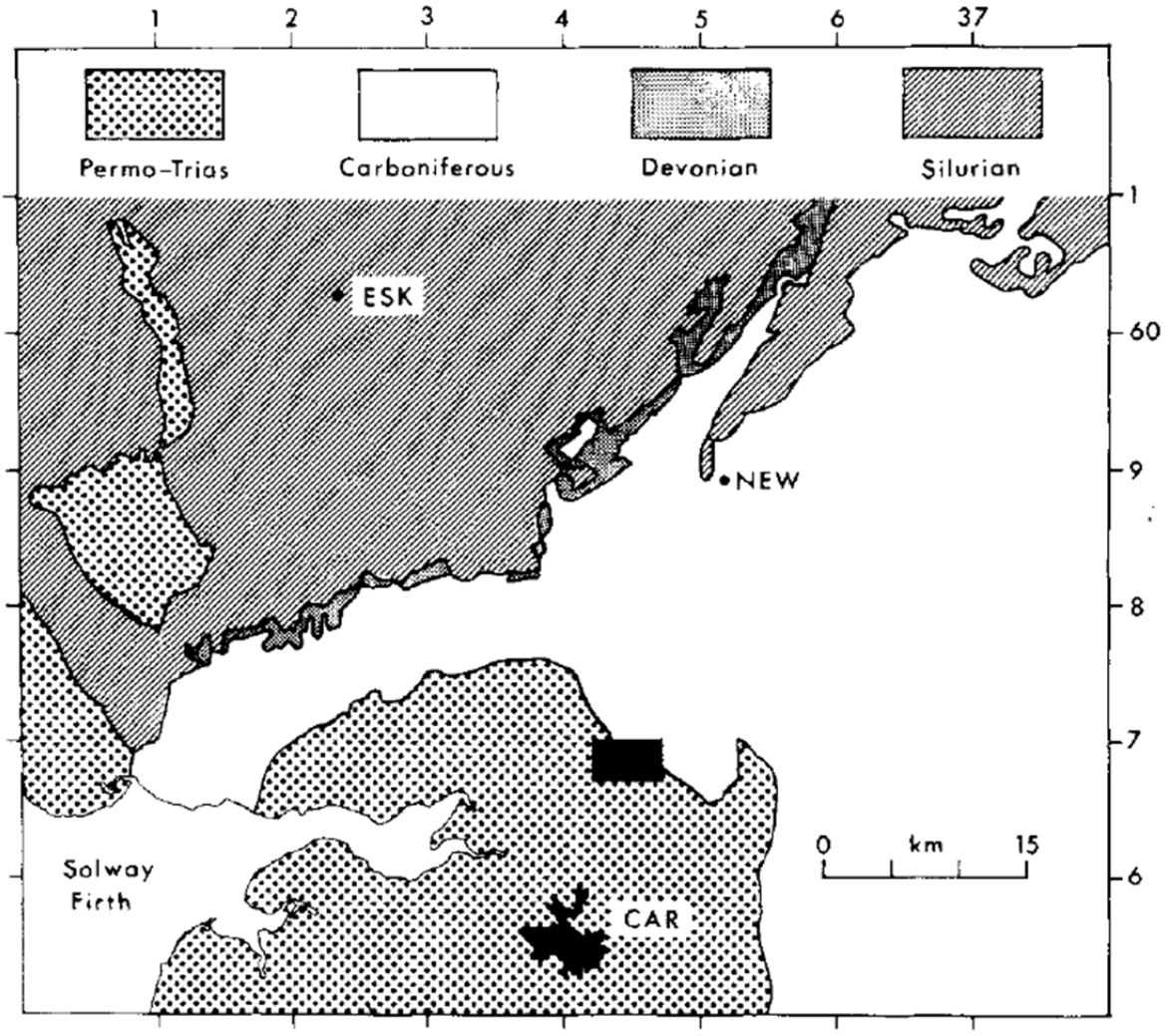

Figure 1. Outline geological sketch map of the earthquake region. The solid rectangle defines an area of epicentral locations obtained with an error of less than 2 km. ESK: Eskdalemuir, NEW: Newcastleton, CAR: Carlisle.

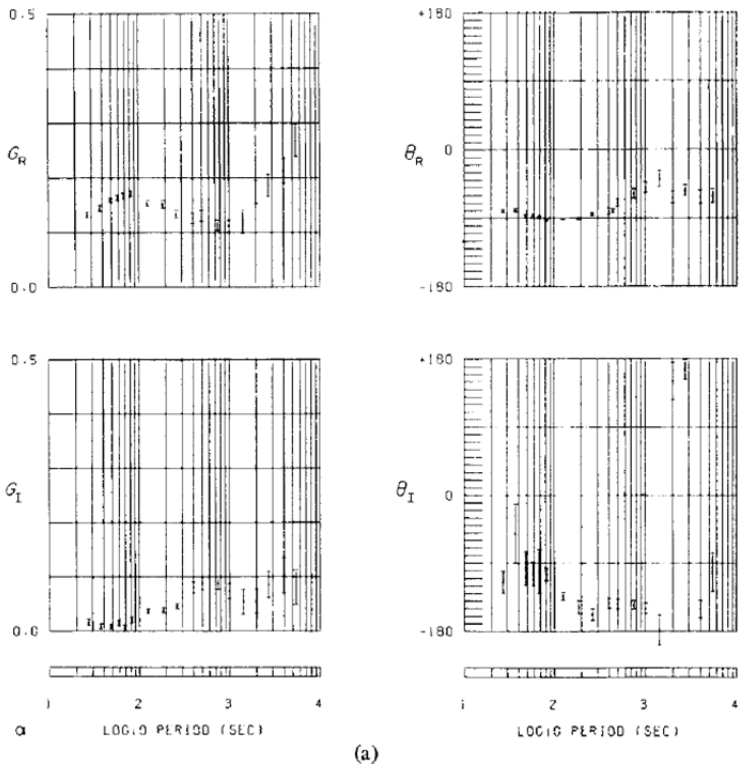

(a)

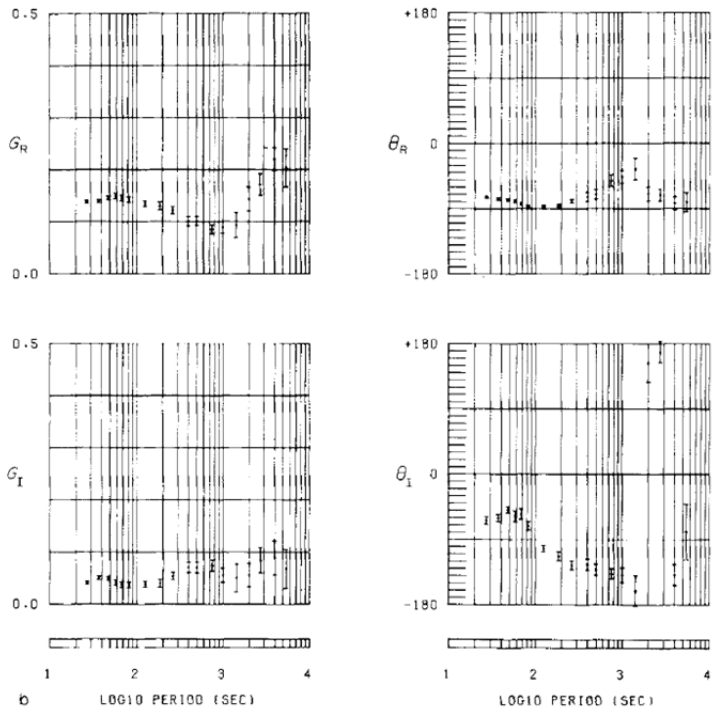

Figure 2 (b)

Figure 2. Real (G_R , θ_R) and imaginary (G_I, θ_I) induction arrows obtained at ESK. (a) Single-station result, using vertical and horizontal fields at ESK. (b) Inter-station result, using vertical field at ESK and horizontal fields at YOR.

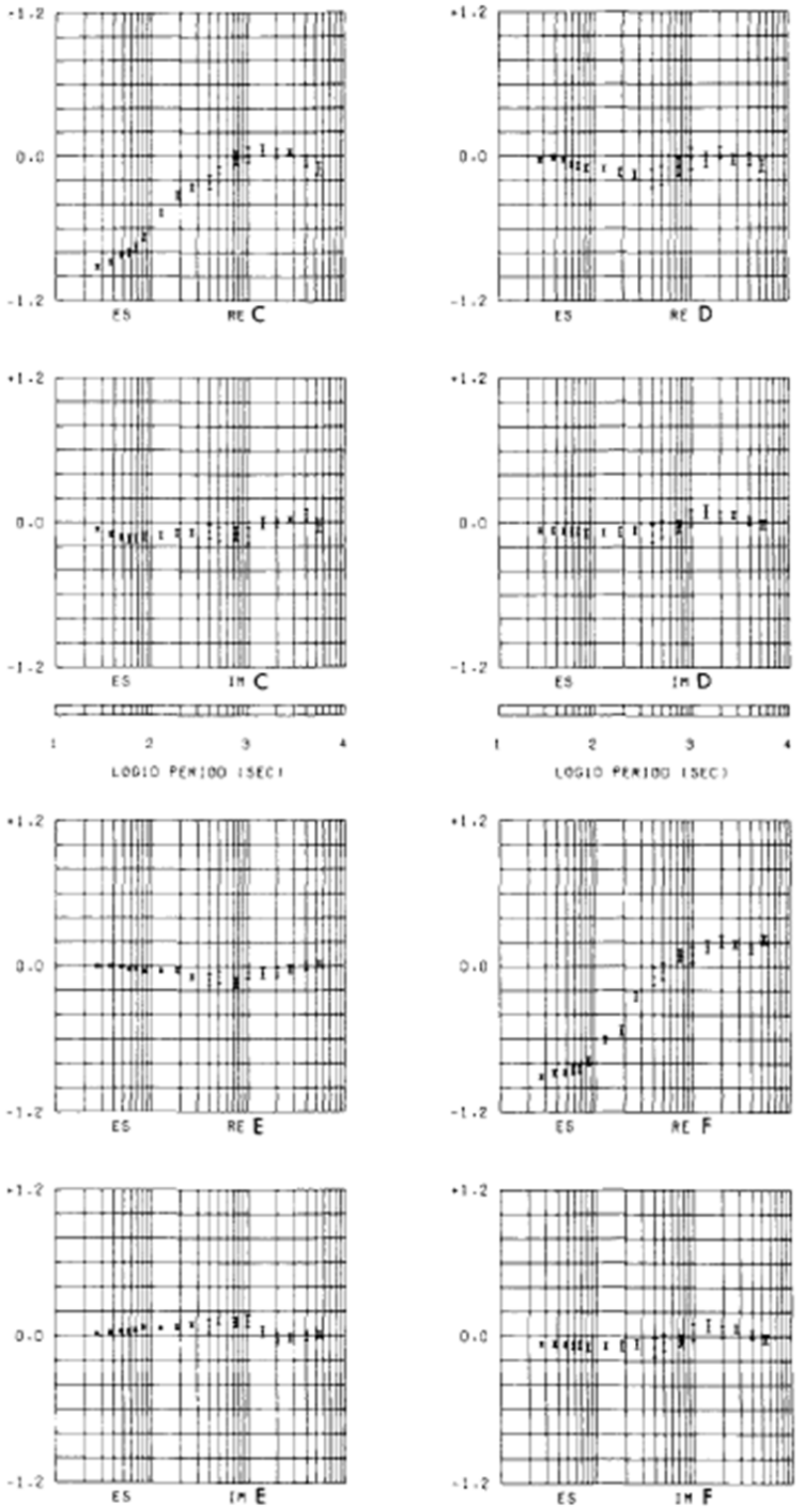

Figure 3. Horizontal field transfer functions (C, D) and (E, F) in terms of real (Re) and imaginary (Im) components, as a function of period. Data centred on day 310 1979.

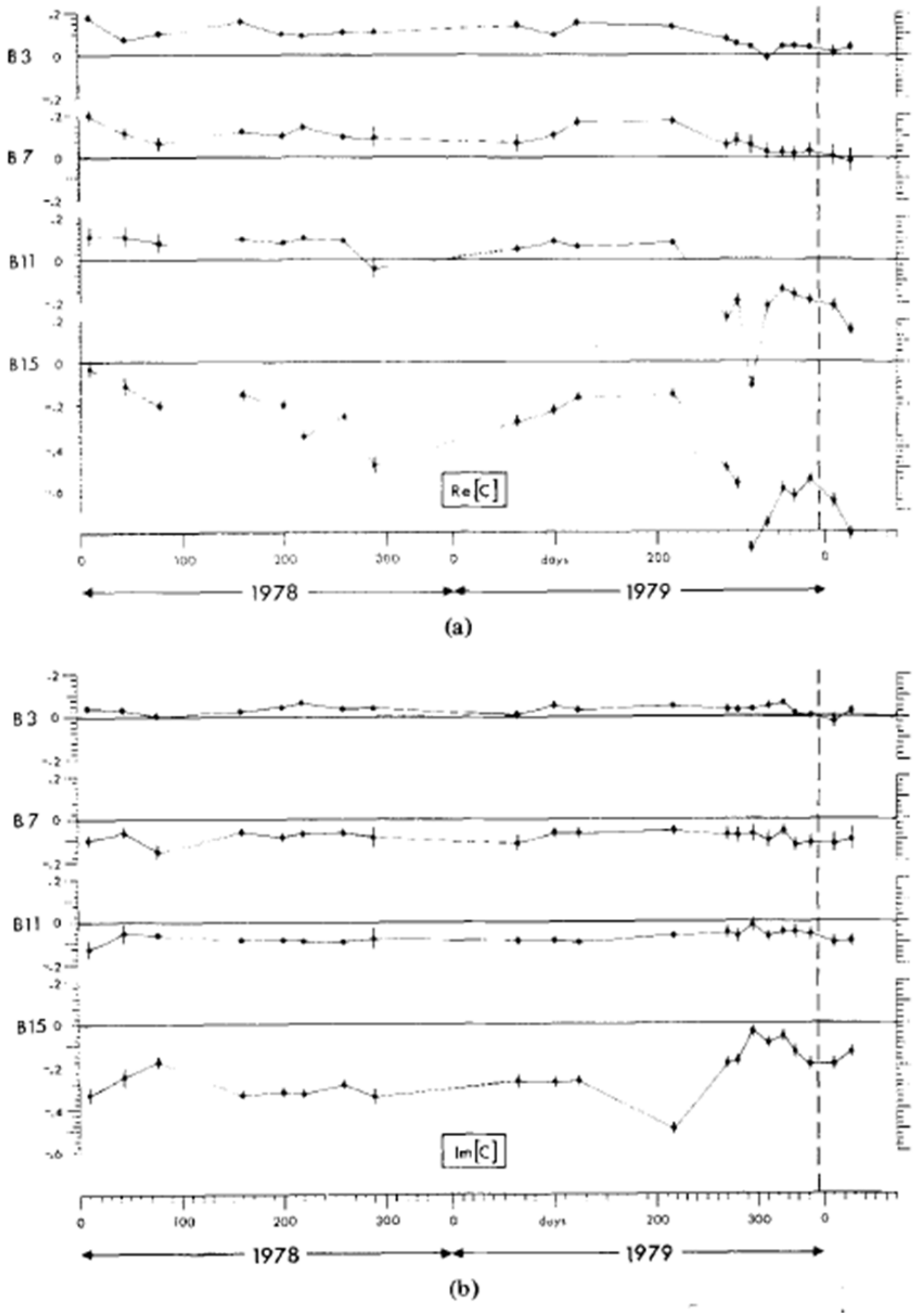

Figure 4. Estimates of inter-station horizontal field transfer function C during 1978 and 1979 for four period ranges: B3 (4000-2000 s), B7 (1000-600 s), B11 (250-150 s) and B15 (70-50 s). (a) In-phase (real) component, (b) In-quadrature (imaginary) component. All error bars are ±1 sd. The occurrence of the Boxing Day earthquake is shown as the broken vertical line.

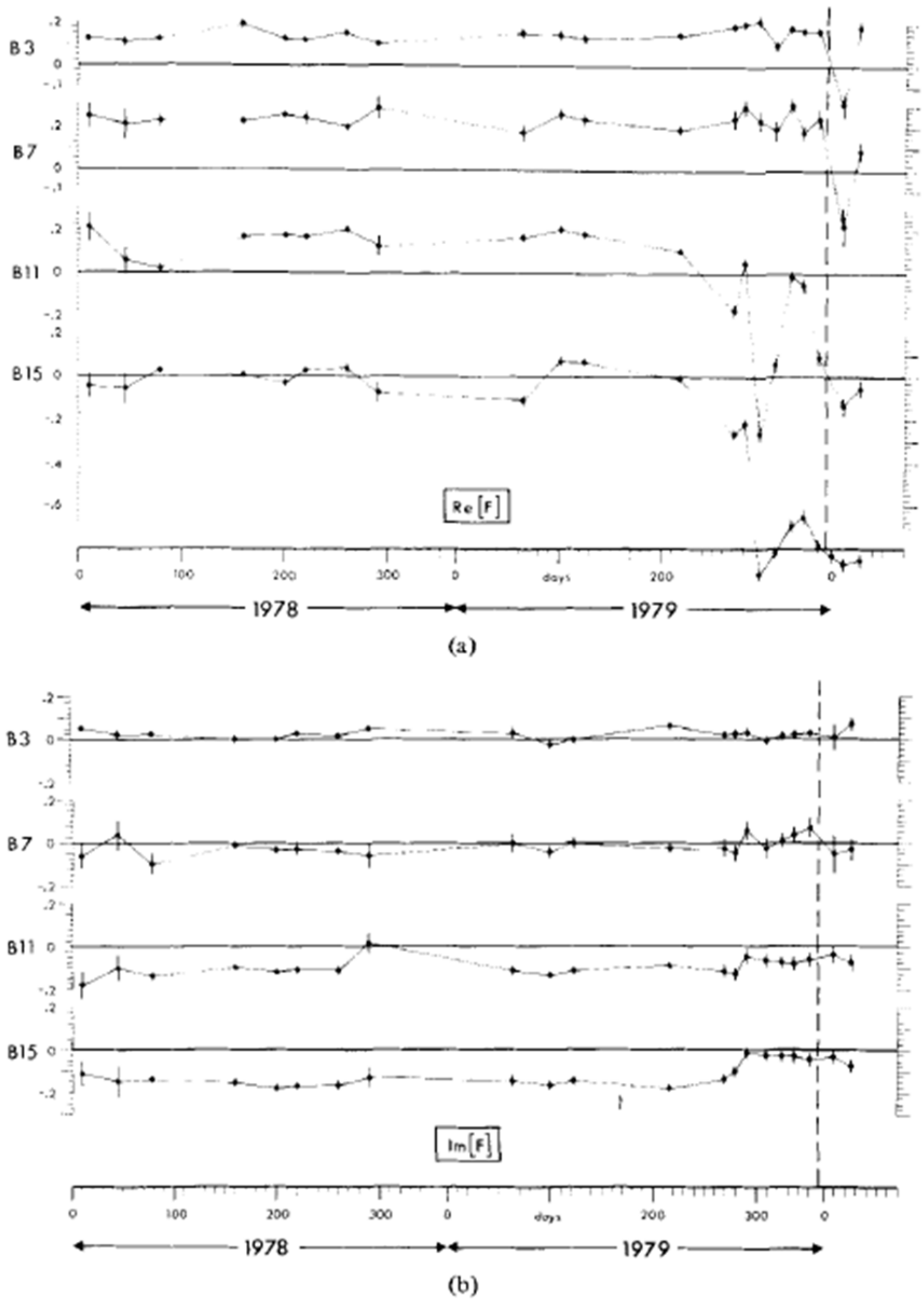

Figure 5. Estimates of inter-station horizontal field transfer function F during 1978 and 1979, and as per Fig. 3.

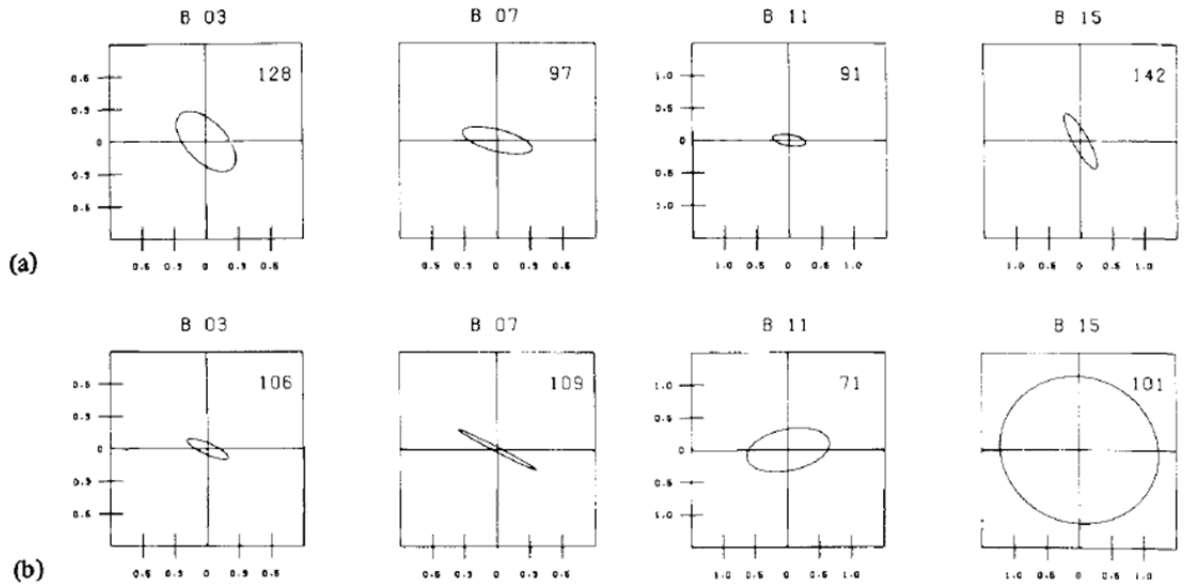

Figure 6. Anomalous horizontal field rotation ellipses for four period ranges and two separate time intervals. (a) Data centred on day 63 1979, (b) Data centred on day 310 1979: the number in the top right corner of each frame refers to the azimuth (clockwise, geographic) of the major axis of the rotation ellipse.